



Targeting TRIM24 promotes neuroblastoma differentiation and decreases tumorigenicity via LSD1/CoREST complex

Qiqi Shi¹ · Bo Yu¹ · Yingwen Zhang¹ · Yi Yang² · Chenxin Xu¹ · Mingda Zhang¹ · Guoyu Chen¹ · Fei Luo¹ · Bowen Sun¹ · Ru Yang¹ · Yanxin Li² · Haizhong Feng¹

Accepted: 7 July 2023 / Published online: 19 July 2023
© Springer Nature Switzerland AG 2023

Abstract

Purpose High-risk neuroblastoma (NB) still has an unfavorable prognosis and inducing NB differentiation is a potential strategy in clinical treatment, yet underlying mechanisms are still elusive. Here we identify TRIM24 as an important regulator of NB differentiation.

Methods Multiple datasets and clinical specimens were analyzed to define the role of TRIM24 in NB. The effects of TRIM24 on differentiation and growth of NB were determined by cell morphology, spheres formation, soft agar assay, and subcutaneous xenograft in nude mice. RNA-Seq and qRT-PCR were used to identify genes and pathways involved. Mass spectrometry and co-immunoprecipitation were used to explore the interaction of proteins.

Results Trim24 is highly expressed in spontaneous NB in TH-MYCN transgenic mice and clinical NB specimens. It is associated with poor NB differentiation and unfavorable prognostic. Knockout of TRIM24 in neuroblastoma cells promotes cell differentiation, reduces cell stemness, and inhibits colony formation in soft agar and subcutaneous xenograft tumor growth in nude mice. Mechanistically, TRIM24 knockout alters genes and pathways related to neural differentiation and development by suppressing LSD1/CoREST complex formation. Besides, TRIM24 knockout activates the retinoic acid pathway. Targeting TRIM24 in combination with retinoic acid (RA) synergistically promotes NB cell differentiation and inhibits cell viability.

Conclusion Our findings demonstrate that TRIM24 is critical for NB differentiation and suggest that TRIM24 is a promising therapeutic target in combination with RA in NB differentiation therapy.

Keywords Neuroblastoma · TRIM24 · LSD1 · Differentiation · Retinoic acid

1 Introduction

Neuroblastoma (NB) is the most common extracranial solid tumor in children and the five-year survival rate of patients with high-risk neuroblastoma is only about 50%

[1, 2]. Retinoic acid (RA) is clinically used as a differentiating agent for high-risk neuroblastoma. However, only a few patients mainly patients with minimal residual disease benefit from RA treatment and the improvement is relatively limited [3, 4]. Thus, there is an urgent need to understand the mechanisms underlying the pathogenesis and differentiation of high-risk neuroblastoma, which may provide new strategies in targeted therapies.

Tripartite motif-containing protein 24 (TRIM24, also called TIF α) is a member of the TRIM family characterized by an N-terminal RING-finger domain, B-box domains, and a coiled-coil domain [5]. Besides, TRIM24 contained a LxxLL motif to bind with nuclear receptors, and a tandem PHD-bromodomain to recognize acetylated H3K23 (H3K23ac) and unmethylated H3K4 (H3K4me0) [6–8]. Therefore, the functions of TRIM24 in tumors are highly context-dependent. TRIM24 exerts oncogenic function in most cancers, including breast cancer, prostate cancer, and

✉ Yanxin Li
liyanxin@scmc.com.cn

✉ Haizhong Feng
fenghaizhong@sjtu.edu.cn

¹ Renji-Med X Clinical Stem Cell Research Center, Ren Ji Hospital, Shanghai Cancer Institute, School of Medicine, State Key Laboratory of Systems Medicine for Cancer, Shanghai Jiao Tong University, Shanghai 200127, China

² Pediatric Translational Medicine Institute, Department of Hematology & Oncology, Shanghai Children's Medical Center, School of Medicine, National Health Committee Key Laboratory of Pediatric Hematology & Oncology, Shanghai Jiao Tong University, Shanghai 200127, China

glioblastoma [8–11]. In addition to working as an E3-ligase to mediate p53 degradation [12], TRIM24 activates an oncogenic pathway transcriptionally by interacting with chromatin and binding with estrogen receptor in breast cancer or androgen receptor in prostate cancer [8, 13]. On the other hand, TRIM24 binds with retinoic acid receptor alpha (RAR α) and inhibits the RA pathway to function as a liver-specific suppressor in mice [14, 15]. However, the role of TRIM24 in tumor cell differentiation is still unknown.

In this study, we first investigated several published datasets and demonstrated that high levels of TRIM24 predicted poor NB differentiation and an unfavorable prognosis for patients. Knockout of TRIM24 promoted cell differentiation and reduced NB tumorigenicity. Then, we found that TRIM24 knockout inhibited LSD1/CoREST complex formation to promote neural gene expression and activated the RA pathway. Finally, targeting TRIM24 in combination with RA treatment enhanced neuroblastoma differentiation.

2 Materials and methods

2.1 Cell lines and cell culture

Human HEK-293 T and NB cell lines SK-N-BE(2), SK-N-AS, SK-N-SH, and SH-SY5Y were from the American Type Culture Collection (ATCC). CHP-134 cells were obtained from the European Collection of Authenticated Cell Cultures (ECACC). CHP-134 was cultured in RPMI1640 with 10% fetal bovine serum. Other cells were cultured in Dulbecco's Modified Eagle Medium (DMEM) supplemented with 10% fetal bovine serum. All cell lines were maintained under standard conditions at 37 °C and 5% CO₂. NB cell lines were authenticated using STR DNA fingerprinting at Shanghai Biowing Applied Biotechnology Co., Ltd. (Shanghai, China) and all cells were periodically checked for mycoplasma contamination.

2.2 Antibodies and reagents

The antibodies against TRIM24 (1:1000, 14,208-1-AP), β -actin (1:5000, 66,009-1-Ig), myc-tag (1:1000, 60,003-2-Ig) were from Proteintech. MYCN (1:1000, #9405), LSD1 (1:1000, #2139), HDAC1 (1:1000, #5356), HA-tag (1:1000, #3724) were from Cell Signaling Technology. Anti-flag antibody (1:1000, F1804) was from Sigma. CoREST (1:200, A3568) was from Abclonal. 13-cis-retinoic acid (HY-15127) was purchased from Med Chem Express.

2.3 Plasmids and transfection

MYCN plasmid was purchased from Addgene (#50772). Flag-TRIM24 was a gift from Michelle Barton (Addgene,

#28138) [8]. Then, TRIM24 was subcloned and inserted into a lentivirus pLenti-blast-HA vector. LSD1 cDNA was amplified from SK-N-BE(2) cDNAs by PCR and cloned into a pLenti-blast-flag vector. For sgRNAs, the oligos were annealed and cloned into a lentiCRISPRv2. The guide RNA sequences targeting TRIM24 were ACACGGCGCAAGTGT CCAA and GGCGGCCCGGCTCAACCTGT. The guide RNA sequence targeting MYCN was CGAGTGC GTGGA TCCCGCCG. shRNA oligos were annealed and cloned into pLKO.1-Puromycin (Puro) or pLKO.1-Blasticidin (Bsd) lentiviral vector. The sense sequence of shLSD1 was GGTTGG ATATCAAGTTAAACA, and the sense sequence of shZIC4 was GCTGAAATCCTGAAAGGCCAT. All plasmids were confirmed by DNA sequencing.

2.4 Generation of stable cell lines

Lentiviruses were produced by co-transfecting plasmids and packaging plasmids into HEK293T cells using Lipofectamine 2000 reagent according to the manufacturer's instruction (#52758, Invitrogen). Forty-eight hours after transfection, the supernatants containing viruses were filtered and added into the culture media supplemented with 8 μ g/ml polybrene. Then infected cells were stably selected using puromycin or blasticidin.

2.5 Immunoprecipitation (IP) and immunoblotting (IB)

Immunoprecipitation and immunoblotting were performed as previously described [16]. Briefly, cells were lysed in immunoprecipitation buffer (20 mM Tris-HCl, pH 7.5, 150 mM NaCl, 1 mM EDTA, 2 mM Na₃VO₄, 5 mM NaF, 1% Triton X-100, and protease inhibitor cocktail) at 4 °C for 30 minutes and then centrifuged for 20 min at 12,000 g. The supernatants were collected and incubated with indicated antibody and protein A/G-agarose beads (Invitrogen). IP beads were then washed with IP lysis buffer and then boiled in SDS loading buffer for further immunoblotting analysis.

2.6 Sphere formation and limited dilution analysis

The single-cell suspension was obtained by trypsinization and then seeded into ultralow attachment 12-well plates at a density of 500 cells/well and cultured in sphere medium (DMEM/F12, 20 ng/ml epidermal growth factor (EGF), 20 ng/ml basic fibroblast growth factor (bFGF), 2% B27, and 5 mg/ml heparin for 2-3 weeks before photograph. For ELDA, cells were seeded into 96-well ultralow attachment 12-well plates at different densities. After 2-3 weeks, neuroblastoma spheres were examined and sphere formation

frequency was calculated using extreme limiting dilution analysis (<http://bioinf.wehi.edu.au/software/elda/>) [17].

2.7 Soft agar colony formation assay

Soft agar assay was performed as previously described [18]. Briefly, cells were seeded in a 0.4% Noble Agar top layer with a bottom layer of 0.8% Difco Noble Agar (BD Biosciences) in each of the triplicate wells of a 12-well plate. Cell culture media was added on the top agar and changed every 3 days. Visible colonies were scored after 2–4 weeks using an Olympus SZX12 stereomicroscope.

2.8 Cell viability

Cell viability was measured using CellTiter-Glo Luminescent Cell Viability Assay according to the manufacturer's instruction (#G7570, Promega). Briefly, cells were seeded in triplicates onto 96-well plates and treated as indicated. CellTiter-Glo reagent was added to each well and incubated at room temperature for 10 minutes. The luminescent signals were measured by GloMax® Discover Microplate Reader (Promega). The cell viability was normalized to the average viability of control wells.

2.9 Mass spectrometry (MS)

Proteomics analyses for TRIM24 binding proteins were performed at Jiyun Biotech. Inc. (Shanghai, China). Briefly, SK-N-BE(2) cells immunoprecipitated with IgG or TRIM24 antibody. The protein samples were analyzed by LC-MS/MS using Q Exactive Plus (Thermo). The raw data were processed by MAXQUANT software. The raw data were searched against the UniProt database.

2.10 Patient samples

The clinical samples were provided by Shanghai Children's Medical Center (SCMC). The study protocol was approved and supervised by the SCMC Ethics Committee, according to the Declaration of Helsinki. All subjects provided written consent for the banking of tissue and future research use of the samples, in accordance with the regulations of the institutional review board of SCMC.

2.11 Quantitative RT-PCR (qRT-PCR)

For quantitative RT-PCR, total RNA was extracted using Trizol reagent (Invitrogen) and reverse-transcribed using the PrimeScript RT reagent Kit (Takara) according to the manufacturer's instructions. The reverse-transcribed cDNAs were used for quantitative PCR analysis using the Power SYBR Green Master Mix (Life Technologies). Results were

analyzed using the $2^{-(\Delta\Delta Ct)}$ method with ACTB expression as an internal control. The primers were listed in Table S1.

2.12 RNA-Seq analysis

Total RNA was extracted and purified using the RNeasy Mini kit (Qiagen) according to the manufacturer's instructions. The quality of RNA was assessed before sequencing. Libraries were generated using the Illumina Truseq strand mRNA Sample Preparation Kit and subjected to the Illumina HiSeqX Ten platform. Raw reads were aligned to hg19 using HISAT2, and reads mapped to genes were counted by featureCounts. Differential gene analysis was performed on gene raw counts in R with an edgeR package. A fold change cut-off of 1.5 and an adjusted *p* value cut-off of 0.05 was used to determine significantly differentially expressed genes. Differentially expressed genes were subjected to gene enrichment analysis with R package clusterProfiler [19]. Gene set enrichment analysis (GSEA) was performed using the Broad GSEA application.

2.13 Animal experiments

All animal experiments were approved by Shanghai Jiao Tong University Institutional Animal Care and Use Committee (IACUC). Six-week-old female nude mice were purchased from Shanghai SLAC Laboratory Animal Co. Ltd., China. Nude mice were randomly divided into three groups. Each group was injected subcutaneously with 5×10^6 either sgCtrl or sgTRIM24 SK-N-BE(2) cells ($n = 6$ mice per group) or CHP-134 cells ($n = 4$ mice per group). Tumor sizes were determined by measuring the length and width every four days. Tumor volumes were calculated according to the following formula: volume (mm^3) = $(\text{length} \times \text{width}^2)/2$. When tumor sizes reached 1500 mm^3 or upon ulceration/bleeding, mice were euthanized, and tumor xenografts were removed and fixed in formalin.

2.14 Immunohistochemical staining

The paraffin-embedded sections were stained with antibodies against TRIM24 (1:1100, 14,208-1-AP, Proteintech), Ki67 (1:200, MA5-14520, Invitrogen) and MAP2 (1:50, #4542, Cell Signaling Technology) as previously described [16]. Images were captured using an Olympus BX53 microscope and processed or quantified using ImageJ by two individuals. Ki-67 was quantified by calculating the percentage of Ki-67 positive cells. The staining for MAP2 and TRIM24 were quantified by four-value proportion score (1, $\leq 25\%$; 2, $>25\%$ and $\leq 50\%$; 3, $>50\%$ and $\leq 75\%$; 4, $>75\%$) plus a staining intensity score (0, negative; 1, weak; 2, intermediate; 3, strong).

2.15 Statistical analysis

Statistical analyses were performed using GraphPad Prism 8.0 software. The results were presented as mean \pm SEM. Two-tailed Student's *t* test was used for comparisons between two groups and one-way ANOVA was used for comparisons between multiple groups. Kaplan-Meier survival analysis was carried out using the log-rank test. Multivariable Cox regression analyses were used to evaluate the risk factors. $P \leq 0.05$ was considered statistically significant.

3 Results

3.1 TRIM24 is highly expressed in neuroblastoma and correlated with unfavorable prognosis

To identify the putative regulators of NB differentiation, we first performed differential expression analysis to estimate the fold change of TRIM family genes between spontaneous NB and dysplastic ganglion in TH-MYCN transgenic mice from the GSE17740 dataset [20] and identified 8 significantly upregulated genes including *Trim24* (Fig. 1a). We confirmed that TRIM24 was significantly higher in spontaneous NB than neural crest-derived adrenal medulla in TH-MYCN transgenic mice through immunohistochemical staining (Fig. 1b). Then, comparing human NB with better-differentiated tumors, ganglioneuroma and ganglioneuroblastoma (GN/GNB), we found that TRIM24 was significantly upregulated in human NB in GSE12460 dataset [21] (Fig. 1c). Additional immunohistochemical staining of NB specimens also demonstrated that TRIM24 levels were positively related with tumor stages (Fig. 1d and e). Besides, TRIM24 was ubiquitously expressed in NB cell lines regardless of MYCN status (Fig. 1f). High TRIM24 expression was associated with worse overall survival in several cohorts including Neuroblastoma Research Consortium (NRC) cohort [22] and SEQC cohort [23] (Fig. 1g). Moreover, high TRIM24 expression was an independent risk factor for shorter overall survival with a hazard ratio of 1.873 by multivariable Cox analysis (Fig. 1h). These data indicate that TRIM24 is ubiquitously and highly expressed in neuroblastoma and is correlated with unfavorable prognosis.

3.2 Knockout of TRIM24 promotes NB cell differentiation and suppresses NB tumorigenicity

Further exploration of the TARGET dataset showed that *TRIM24* expression was higher in poorly or undifferentiated NB than that in differentiated NB (Fig. 2a). We also detected the mRNA levels of *TRIM24* in clinical specimens and *TRIM24* was indeed significantly higher in the

undifferentiation group (Fig. 2b). Since *TRIM24* expression showed no obvious relation with MYCN expression (Fig. 2c-e), we suspect that *TRIM24* expression was negatively related with NB differentiation state and independent of MYCN. We established *TRIM24* knockout (KO) cells using two sgRNAs in MYCN-amplified CHP-134 and SK-N-BE(2) cells and MYCN-non-amplified SH-SY5Y cells (Fig. 2e and Fig.S1a). As expected, we found that *TRIM24* KO significantly increased neurite outgrowth in CHP-134 and SK-N-BE(2) cells (Fig. 2f and g) as well as in SH-SY5Y cells (Fig. S1b and S1c). Consistently, *TRIM24* KO upregulated the expression of various differentiation-related marker genes, such as NEFM, NF68, TH, and TRKA (Fig. 2h and Fig. S1d) in these cells. Besides, *TRIM24* KO-induced NB cell differentiation was accompanied by decreased NB sphere formation (Fig. 2i and j). These results demonstrate that *TRIM24* KO promotes NB cell differentiation independent of MYCN.

Next, we examined the effects of *TRIM24* KO on NB cell growth and tumorigenicity using soft agar assays and subcutaneous xenograft animal models. As shown in Fig. 3a and b, *TRIM24* KO reduced anchorage-independent colony formation of CHP-134 and SK-N-BE(2) cells. Furthermore, *TRIM24* KO significantly decreased tumor growth and tumor weight of SK-N-BE(2) cells (Fig. 3c-e). Similarly, *TRIM24* KO reduced CHP-134 xenograft tumorigenicity (Fig. 3f-h). Further immunohistochemistry staining showed decreased proliferation rates and increased differentiation assessed by Ki-67 and MAP2 (Fig. 3i-k). Taken together, these data demonstrate that targeting *TRIM24* promotes NB differentiation and decreases tumorigenicity.

3.3 TRIM24 knockout up-regulates genes involved in neural differentiation pathways

To gain insight into the molecular mechanism of *TRIM24* KO-induced NB differentiation, we performed RNA-Seq in CHP-134 cells. As shown in Fig. 4a, *TRIM24* KO significantly up-regulated 991 genes and down-regulated 512 genes (fold change ≥ 1.5 , adjusted $P \leq 0.05$). Further Gene Ontology (GO) enrichment analysis showed that both upregulated and downregulated differentially expressed genes were enriched in pathways related to neural development and differentiation (Fig. 4b). Gene set enrichment analysis (GSEA) also suggested significant enrichment of neural differentiation-related gene signatures in *TRIM24* KO CHP-134 cells (Fig. 4c). qRT-PCR analysis confirmed that *TRIM24* KO in SK-N-BE(2), CHP-134, and SH-SY5Y cells significantly increased the expressions of several genes known to be related to neural differentiation and NB differentiation [24, 25], including ZIC4, CLU, and CDKN1A (Fig. 4d). These data suggest that *TRIM24* KO upregulates differentiation-related genes to promote NB differentiation.

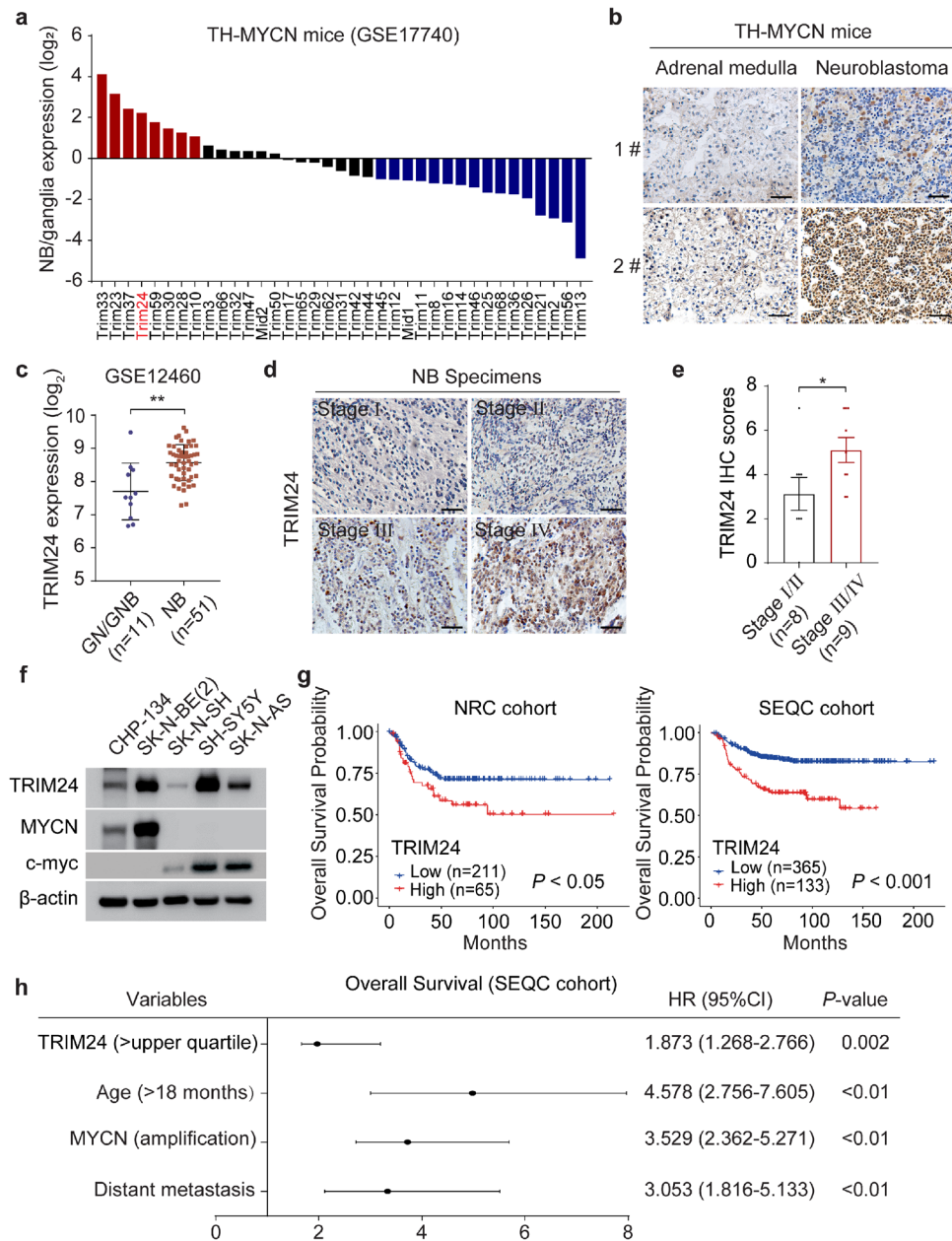
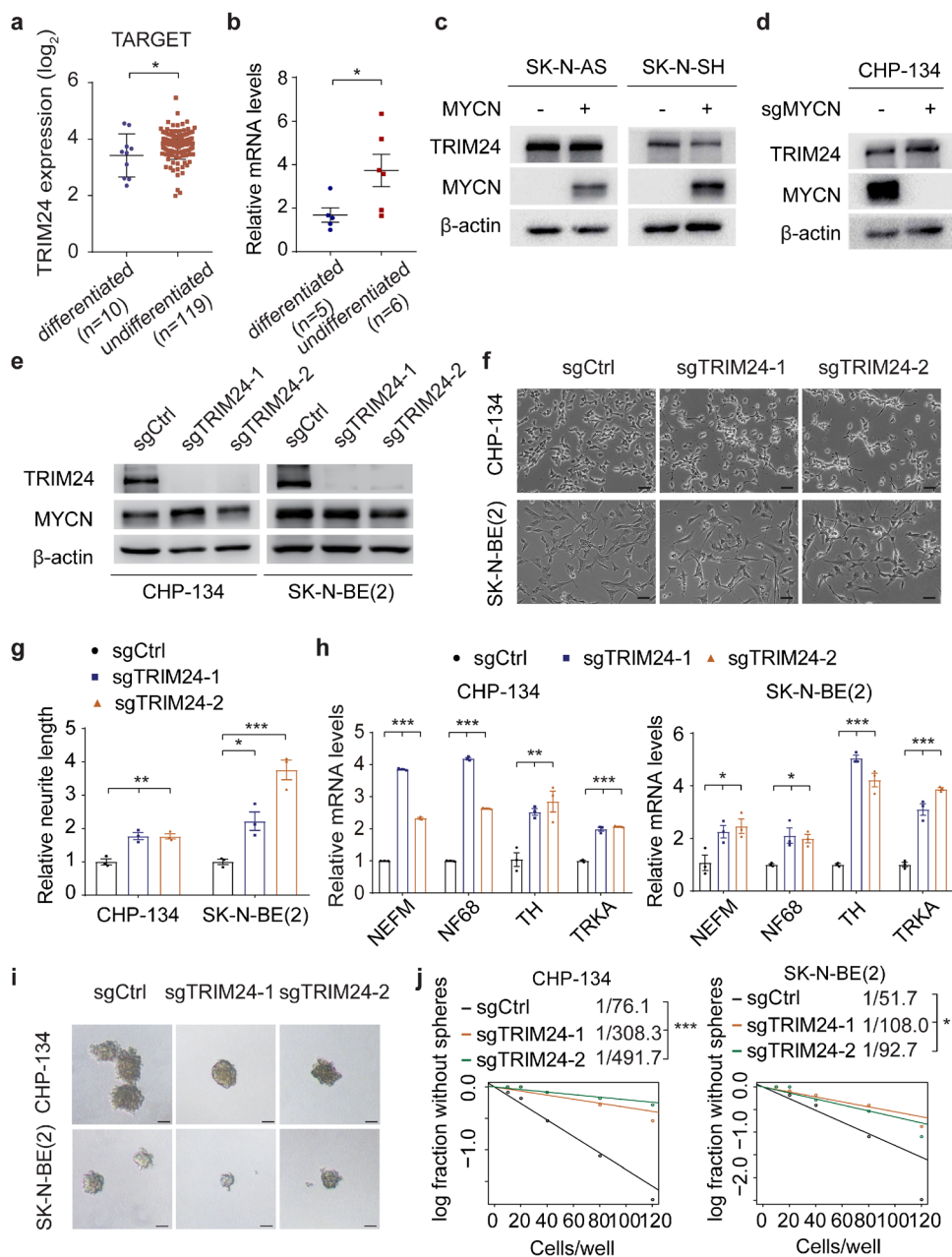


Fig. 1 TRIM24 is highly expressed in neuroblastoma and is correlated with unfavorable prognosis **(a)** Barplot showing the log₂ transformed fold-change of TRIM family genes expression in spontaneous neuroblastoma ($n = 26$) comparing with hyperplastic ganglia ($n = 9$) from TH-MYCN transgenic mice in GSE17740 dataset. Fold-change ≥ 1.5 and adjusted p value ≤ 0.05 were applied as cutoffs. Red indicated significantly upregulated and blue indicated significantly downregulated in neuroblastoma. **(b)** Representative images of immunohistochemistry staining showed TRIM24 expression in the adrenal medulla and spontaneous neuroblastoma from two TH-MYCN transgenic mice. Scale bars, 50 μ m. **(c)** Plot displayed the expression of TRIM24 in human neuroblastoma (NB) and ganglioneuroma/ganglioneuroblastoma (GN/GNB) from GSE12460 dataset ($n = 62$).

(d) Representative images of immunohistochemistry staining showed TRIM24 levels in neuroblastoma specimens from patients with different stages. Scale bars, 50 μ m. **(e)** Quantification of TRIM24 expression in **(d)**. **(f)** Identification of TRIM24 expression in neuroblastoma cell lines by immunoblotting. **(g)** Kaplan-Meier analysis of overall survival in neuroblastoma patients with high or low expression of TRIM24 from the NRC cohort (GSE85047) and SEQC cohort (GSE62564). The best cut-point was employed as the cutoff. **(h)** Forest plot showed the hazard ratio (HR) with 95% confidence intervals (CI) of the association of overall survival and TRIM24 expression in the SEQC cohort (GSE62564). Data were presented as mean \pm SEM. * $P \leq 0.05$, ** $P \leq 0.01$, *** $P \leq 0.001$, by two-tailed Student's t test or log-rank test or Cox multivariate analysis

Fig. 2 Knockout of TRIM24 promotes neuroblastoma cell differentiation independent of MYCN (a) Plot displayed the expression of TRIM24 in differentiated and poorly differentiated or undifferentiated neuroblastoma from the TARGET dataset ($n = 129$). b The relative mRNA level of TRIM24 in differentiated and undifferentiated neuroblastoma specimens ($n = 11$) was determined by qRT-PCR analysis. c-d Effects of overexpression of MYCN in SK-N-AS and SK-N-SH cells (c) or knockout of MYCN in CHP-134 cells (d) on TRIM24 expression were determined by immunoblotting. e Validation of TRIM24 and MYCN expression in control and TRIM24-KO CHP-134 and SK-N-BE(2) cells by immunoblotting. f-g The morphology changes (f) and quantification of neurite lengths (g) of CHP-134 and SK-N-BE(2) after TRIM24 KO. Scale bars, 50 μm . h Relative mRNA levels of indicated neural differentiation marker genes upon TRIM24 KO were determined by qRT-PCR analysis. i The representative images of neuroblastoma spheres. Scale bars, 50 μm . j Limiting dilution sphere-forming assays in CHP-134 and SK-N-BE(2) cells and corresponding TRIM24 KO cells. Data were representative of three independent experiments with similar results. Data were presented as mean \pm SEM. * $P \leq 0.05$, ** $P \leq 0.01$, *** $P \leq 0.001$, by two-tailed Student's t test



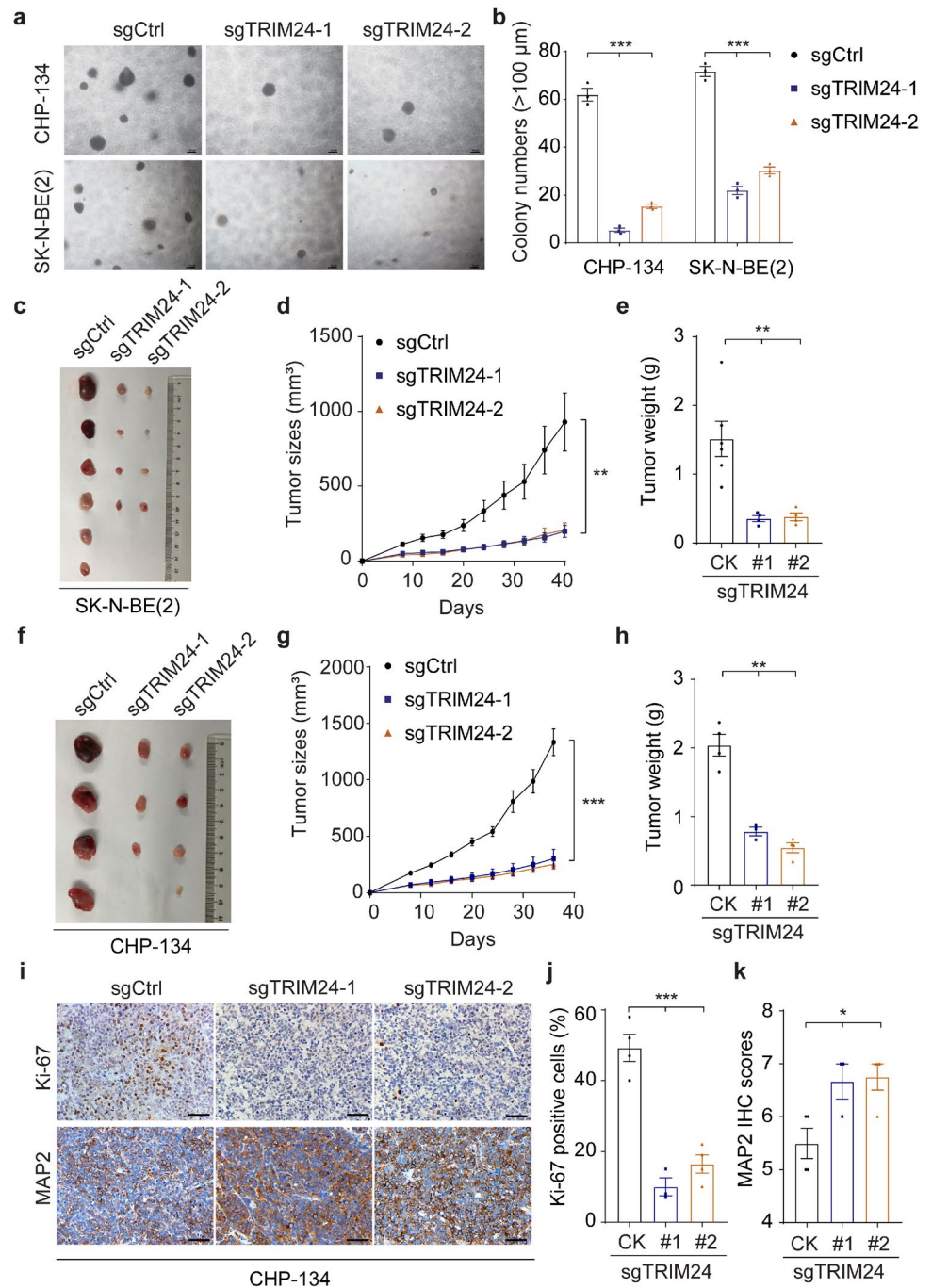
3.4 TRIM24 knockout disrupts LSD1-CoREST complex formation to promote differentiation

To investigate the underlying mechanism of NB differentiation regulated by TRIM24, we performed immunoprecipitation and mass spectrometry in SK-N-BE(2) cells to identify the interaction partners of TRIM24. We detected several components of the LSD1-CoREST transcriptional repression complex, including LSD1, CoREST, and HDAC1/2 (Fig. 5a).

The LSD1-CoREST complex is unique in containing both demethylase LSD1 and deacetylase HDAC1 [26]. By forming a complex, CoREST allows the crosstalk between

deacetylation and demethylation, and tethers LSD1 to the nucleosomes to demethylate H3K4, resulting in repression of neural gene transcription [26–29]. Moreover, its core component LSD1 has been proven to be overexpressed in poorly differentiated NB and impeded NB differentiation by inhibiting neural gene transcription such as PAX3, and ZIC4 [24, 30]. We validated exogenous TRIM24 interaction with LSD1 in HEK-293 T (Fig. 5b) and endogenous TRIM24 interaction with LSD1-CoREST complex components including LSD1, CoREST, and HDAC1 in SK-N-BE(2) cells by immunoprecipitation (Fig. 5c). We further hypothesized that TRIM24 might be involved in LSD1-CoREST complex expression or formation. To this end, we

Fig. 3 Knockout of TRIM24 reduces colony formation and inhibits neuroblastoma tumorigenicity **(a)** Representative areas from anchorage independent growth of control and *TRIM24*-KO CHP-134 and SK-N-BE(2) cells in soft agar assays. Scale bars, 200 μ m. **b** Quantification of soft agar colonies with diameters greater than 100 μ m in **(a)**. **c** and **f** Tumor masses of indicated SK-N-BE(2) xenografts ($n = 6$ mice per group) **(c)** and CHP-134 xenografts ($n = 4$ mice per group) **(f)**. **d** and **g** Tumor growth curves of indicated SK-N-BE(2) xenografts **(d)** and CHP-134 xenografts **(g)** in nude mice. **e** and **h** Tumor weights of indicated SK-N-BE(2) tumors **(e)** and CHP-134 tumors **(h)**. CK indicated control group. **i** Representative images of immunohistochemistry staining showed proliferation index Ki-67 and neuronal differentiation marker MAP2 expression in CHP-134 xenografts. Scale bars, 50 μ m. **j** and **k** Quantification of Ki-67 positive cells **(j)** and MAP2 IHC score **(k)** in indicated CHP-134 tumors. Data were presented as mean \pm SEM. * $P \leq 0.05$, ** $P \leq 0.01$, *** $P \leq 0.001$, by two-tailed Student's *t* test

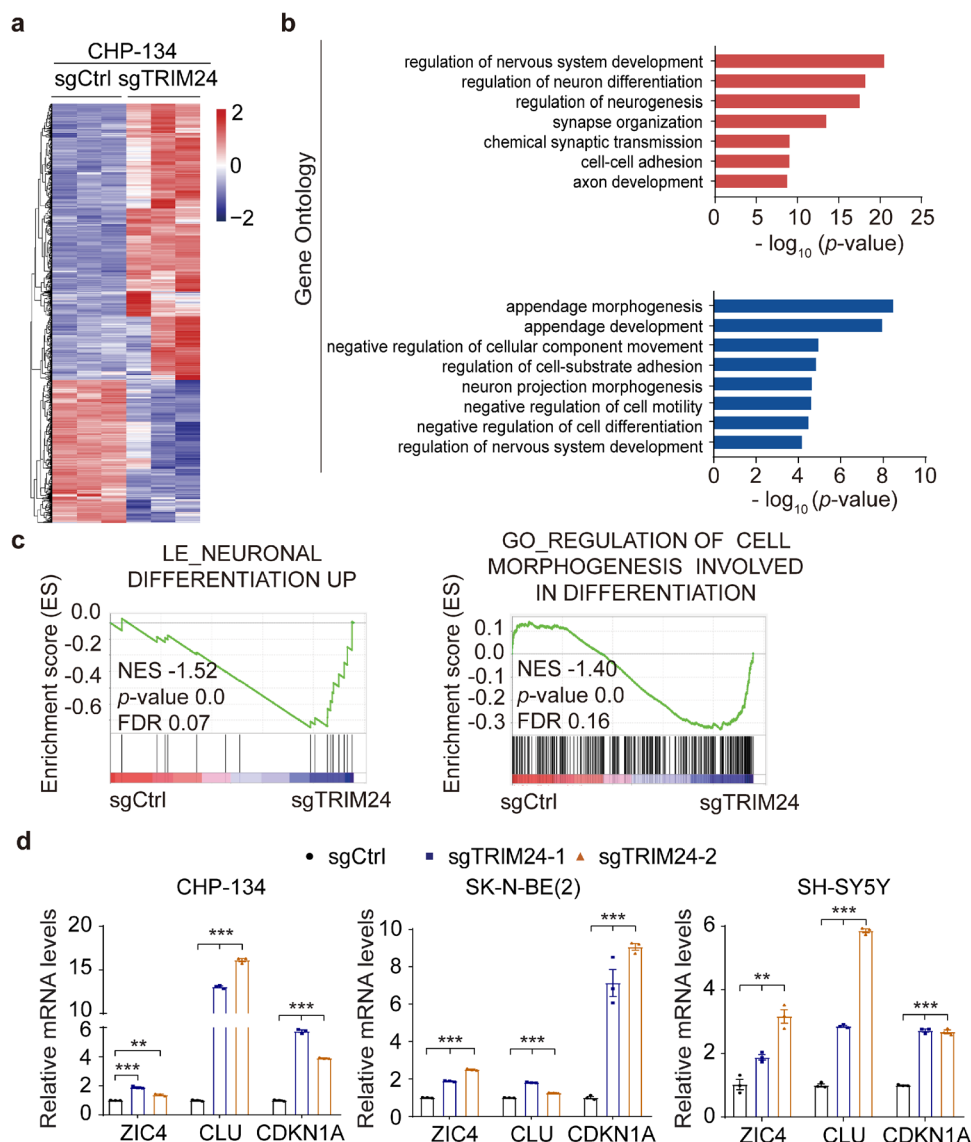


detected LSD1 interaction with HDAC1 and CoREST in control and *TRIM24*-KO SK-N-BE(2) cells. As shown in Fig. 5d, after *TRIM24* KO, LSD1 binding with CoREST and HDAC1 was markedly weakened while their expressions were not affected.

Next, we stably knocked down LSD1 in control and *TRIM24*-KO SK-N-BE(2) cells to further explore the relationship of TRIM24 and LSD1 in NB (Fig. 5e). As shown in Fig. 5f, compared with *TRIM24* KO or *LSD1*

knockdown (KD) alone, knocking down LSD1 in *TRIM24*-KO cells further induced the expression of CDKN1A and ZIC4. Knocking down ZIC4 in *TRIM24*-KO SK-N-BE(2) cells repressed *TRIM24* KO-upregulated neural differentiation marker genes (Fig. 5g), indicating that ZIC4 functioned as one of the downstream effectors of TRIM24 in NB differentiation. Taken together, our data demonstrate that targeting TRIM24 promotes NB differentiation via the LSD1-CoREST complex.

Fig. 4 TRIM24 knockout up-regulates neuroblastoma differentiation pathways (a) Clustering heatmap showed differentially expressed genes between TRIM24-KO and control CHP-134 cells. **b** Gene ontology (GO) enrichment analysis of significantly upregulated genes (red) and downregulated genes (blue). **c** Gene set enrichment analysis (GSEA) showed enrichment of neuronal differentiation-related gene signatures in TRIM24-KO CHP-134 cells. NES, normal enrichment score. **d** Relative mRNA levels of ZIC4, CLU, and CDKN1A in control and TRIM24-KO CHP-134, SK-N-BE(2), and SH-SY5Y cells were determined by qRT-PCR analysis. Data were representative of three independent experiments with similar results. Data were presented as mean \pm SEM. * $P \leq 0.05$, ** $P \leq 0.01$, *** $P \leq 0.001$, by two-tailed Student's t test

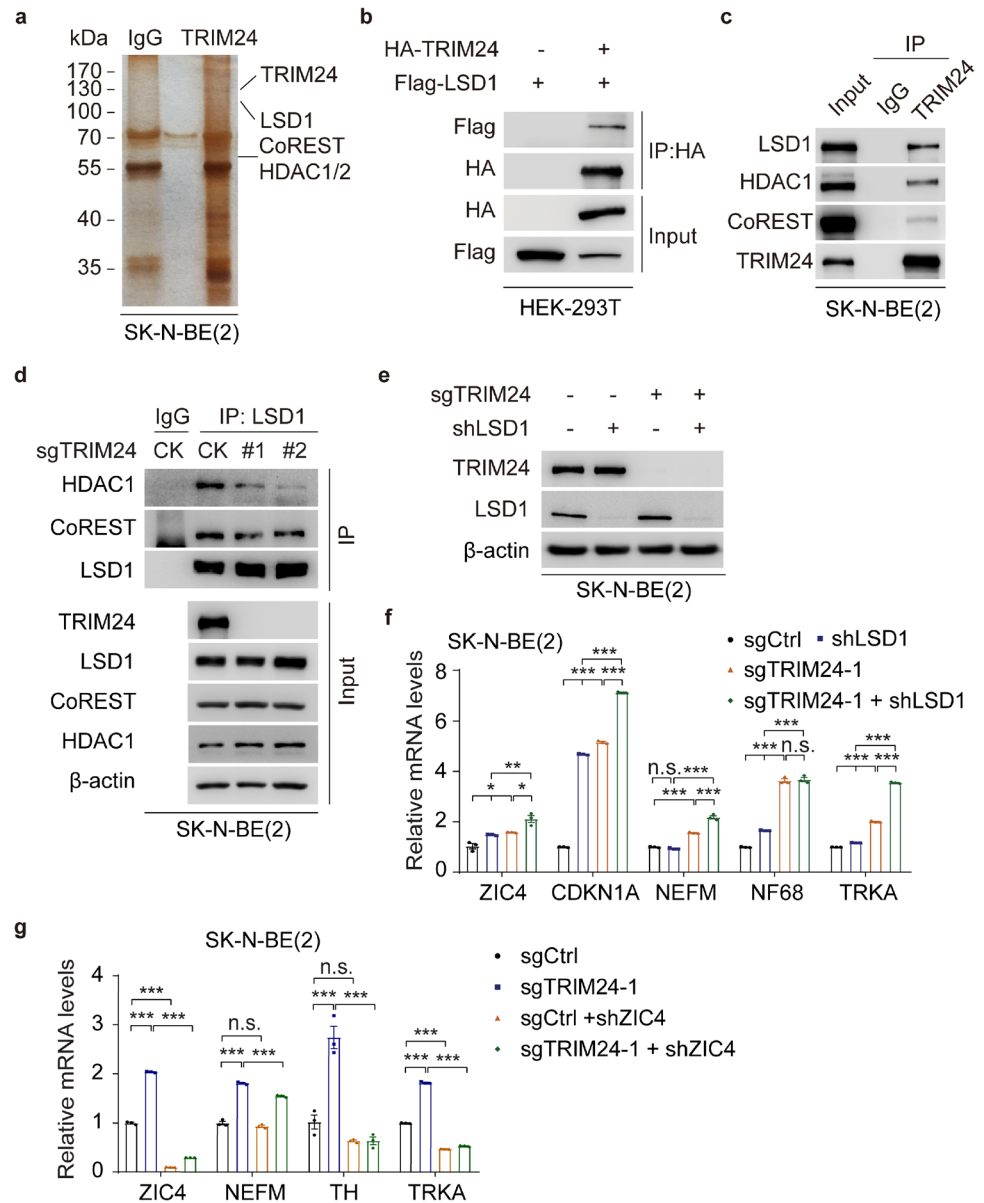


3.5 Targeting TRIM24 in combination with retinoic acid promotes NB differentiation

Previous studies demonstrated that TRIM24 inhibits the retinoic acid (RA) pathway to function as a liver-specific suppressor in mice [14, 15], and LSD1 or HDAC1 inhibitors exhibit synergy with RA treatment in NB [31, 32]. Thus, we first assessed whether TRIM24 KO regulated RA-related pathways and found that RA-related pathways were significantly enriched in TRIM24 KO CHP-134 cells using GSEA (Fig. 6a), indicating that TRIM24 KO activates the RA pathway. In addition, we found that a considerable number of known RA pathway downstream genes, including direct RA targets RBP1, TGM2, and STRA6 as well as downstream responder CDKN1A [14, 24], were significantly up-regulated in TRIM24 KO cells in our RNA-seq

data (Figs. 4d and 6b). Further qRT-PCR analysis results validated that TGM2 and RBP1 mRNA levels were significantly increased after TRIM24 KO (Fig. 6c) in all cell lines used. Next, we examined whether targeting TRIM24 could enhance the effect of RA. Compared with TRIM24 KO or RA treatment alone in SK-N-BE(2) cells, TRIM24 KO in combination with RA treatment synergistically increased neurite outgrowth and upregulated the expression of neural differentiation marker genes (Fig. 6d-f). Besides, TRIM24 KO or RA treatment alone reduced cell viability in SK-N-BE(2) and SH-SY5Y cells, while TRIM24 KO combined with RA treatment synergistically decreased cell viability (Fig. 6g). These data indicate that targeting TRIM24 in combination with RA treatment induces NB differentiation, suggesting that this may be a potential therapeutic strategy.

Fig. 5 TRIM24 knockout disrupts LSD1-CoREST complex formation (a) Silver staining showed the associated proteins of TRIM24 in SK-N-BE(2) cells identified by immunoprecipitation (IP) and mass spectrometry. (b) Co-immunoprecipitation (Co-IP) analysis of exogenous HA-TRIM24 and Flag-LSD1 interaction in HEK293T cells. (c) Co-IP analysis identified the interaction of endogenous TRIM24 with LSD1, CoREST and HDAC1 in SK-N-BE(2) cells. (d) Effects of TRIM24 KO on the assembling of LSD1, HDAC1 and CoREST. (e) Validation of LSD1 knockdown in control and *TRIM24*-KO SK-N-BE(2) cells by immunoblotting. CK: Control knockout cells. (f) Effects of LSD1 knockdown on the mRNA levels of *ZIC4* and *CDKN1A* and neural differentiation marker genes in control and *TRIM24*-KO SK-N-BE(2) cells. (g) qRT-PCR analysis of the mRNA levels of *ZIC4* and neural differentiation marker genes upon *ZIC4* knockdown in control and *TRIM24*-KO SK-N-BE(2) cells. Data were representative of three independent experiments with similar results. Data were presented as mean \pm SEM. * $P < 0.05$, ** $P < 0.01$, *** $P < 0.001$, by two-tailed Student's *t* test or one-way ANOVA analysis



4 Discussion

In the treatments for high-risk NB patients, RA is commonly used in maintenance therapy to reduce the risk of recurrence after high-dose chemotherapy or transplantation, but the effectiveness is limited and it only slightly improves the 5-year overall survival rate [3, 4]. Therefore, it is urgent to find new therapeutic targets and explore the synergistic effect while combining with RA treatment. Here we demonstrate that targeting TRIM24 in combination with RA treatment synergistically promotes NB differentiation.

In this study, we show that TRIM24 has a new function as a critical regulator of NB differentiation. TRIM24 has been demonstrated to function as an oncogene in breast cancer, prostate cancer and glioblastoma [8–11]. Meanwhile, it was

also reported to work as a liver-specific tumor suppressor in mice [14, 15]. In our study, knockout of TRIM24 significantly promoted NB cell differentiation in vitro and reduced NB tumorigenicity in soft agar assay and xenograft animal model. High TRIM24 expression is associated with the undifferentiation state of NB and poor outcomes in patients.

Here, we demonstrate that *TRIM24* KO promotes NB differentiation through suppressing LSD1/CoREST complex formation. The complex functions as a transcription repressor to suppress neural differentiation by epigenetic silencing. CoREST binds with LSD1 and further promotes LSD1 associating with nucleosomes to demethylate H3K4me1/2 and inhibit downstream transcription [26, 28, 29, 33]. LSD1 inhibition was found to activate RA pathways by regulating H3K4me1/2 enrichment in

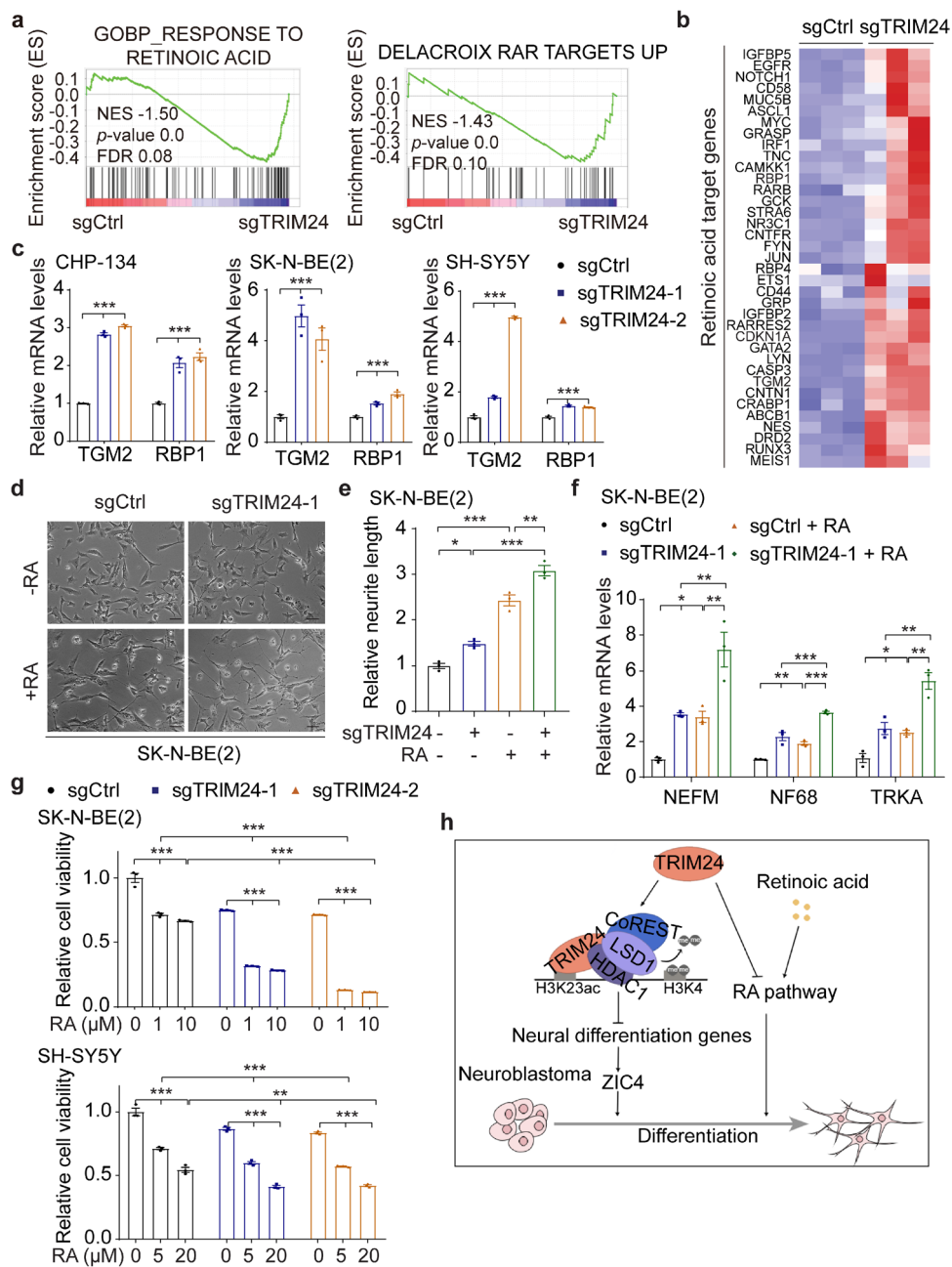


Fig. 6 Targeting TRIM24 in combination with retinoic acid therapy promotes neuroblastoma differentiation **(a)** GSEA showed enrichment of retinoic acid-related pathways in *TRIM24*-KO cells. **(b)** Heatmap showed RNA-seq analysis of known retinoic acid pathway targets significantly upregulated in *TRIM24*-KO CHP-134 cells. **(c)** Relative mRNA levels of RBP1 and TGM2 in control and *TRIM24*-KO CHP-134, SK-N-BE(2), and SH-SY5Y cells were determined by qRT-PCR analysis. **(d)** and **(e)** The morphology changes **(d)** and quantification of neurite lengths **(e)** of SK-N-BE(2) cells after *TRIM24* KO in the absence or presence of RA (10 μ M) for 7 days. Scale bars, 50 μ m. **(f)** qRT-PCR analysis of the mRNA levels of neural differentiation marker genes upon RA (10 μ M) treatment for 7 days in control and *TRIM24*-KO SK-N-BE(2) cells. **(g)** Relative cell viability of

control and *TRIM24*-KO SK-N-BE(2) and SH-SY5Y cells treated with DMSO or indicated RA for 7 days. **(h)** Schematic illustration of TRIM24 inhibiting neuroblastoma differentiation and promoting oncogenesis through binding with LSD1. TRIM24 promotes LSD1 and HDAC1, CoREST complex formation in neuroblastoma cells to inhibit the expression of neural differentiation genes such as ZIC4. Besides, TRIM24 inhibits the RA pathway. Altogether, TRIM24 inhibits neuroblastoma differentiation and promotes tumorigenesis. Data were representative of three independent experiments with similar results. Data were presented as mean \pm SEM. * $P \leq 0.05$, ** $P \leq 0.01$, *** $P \leq 0.001$, by two-tailed Student's *t* test or one-way ANOVA analysis

acute myeloid leukemia [34]. LSD1 also demethylated H3K4me1/2 on the promoters of neural genes such as PAX3, and ZIC4 and inhibited NB differentiation [24]. In addition, inhibition of LSD1 or a further combination of LSD1 inhibitors and RA treatment promoted NB differentiation [30, 32]. Our results showed that *LSD1* KD promoted *TRIM24* KO-induced differentiation and the knockdown of LSD1 known target ZIC4 attenuated *TRIM24* KO-induced differentiation. Besides, *TRIM24* KO in NB activated the RA pathway which was consistent with a previous finding that TRIM24 inhibited the RA signaling pathway in animal liver cancer models [7, 14, 35]. Our study suggests that *TRIM24* KO disrupts LSD1/CoREST complex to activate neural differentiation genes meanwhile it activates the RA pathway and finally promotes NB differentiation. However, the crosstalk of pathways and molecular insight warrant further investigation.

In this study, we also show that targeting TRIM24 in combination with RA treatment is a potential therapeutic strategy for NB. Two small molecule inhibitors targeting TRIM24, namely TRIM24 bromodomain inhibitor IACS-9571 [36] and VHL-ligand-based proteolysis targeting chimera (PROTAC) dTRIM24 [37] have been used to treat various tumors in vitro [38, 39]. It is putative to treat high-risk NB with these inhibitors combined with RA.

In conclusion, our findings identify TRIM24 as a critical regulator of NB differentiation, and targeting TRIM24 with RA treatment promotes NB differentiation via LSD1/CoREST complex, suggesting that TRIM24 may serve as a new prognostic factor and a novel therapeutic target for NB differentiation therapy.

Supplementary Information The online version contains supplementary material available at <https://doi.org/10.1007/s13402-023-00843-4>.

Author contributions H.F. and Y.L. designed and supervised the project. Q.S., B.Y., Y.Z., Y.Y., and G.C. performed experiments. Q.S., Y.L., and H.F. interpreted and/or reviewed the data and wrote the manuscript. C.X., M.Z., F.L., B.S., and R.Y. edited the manuscript. All authors contributed to the article and approved the final manuscript.

Funding This work was supported in part by the National Natural Science Foundation of China (82072896 to H.F., 81972341 and 32271007 to Y. Li, 82103657 to B.S., 82173356 and 81972343 to R.Y.); Program of Shanghai Academic/Technology Research Leader (21XD1403100), and Shanghai Municipal Education Commission-Gaofeng Clinical Medicine Grant (20161310) to H.F.; the Shanghai Municipal Science and Technology Commission (201409002700 and 23ZR1441000 to Y.Li. and 21ZR1439500 to F.L.); and the State Key Laboratory of Oncogenes and Related Genes (KF2115) to F.L.

Data availability RNA-Seq data reported in this study have been deposited with the Gene Expression Omnibus under the accession GEO ID: GSE227066. The datasets analyzed supporting the results of this study are available in the Gene Expression Omnibus and Therapeutically Applicable Research to Generate Effective Treatments (TARGET) program.

Declarations

Ethics statement The study was conducted according to the Ethical Principles of Measures for Ethical Review of Biomedical Research Involving Human Beings and the Declaration of Helsinki.

Consent to participate All patients provided written informed consent prior to participating in any study-specific procedures.

Consent for publication All authors read and approved the final manuscript.

Competing interests All authors declare no conflict of interest.

References

1. S.L. Cohn, A.D. Pearson, W.B. London, T. Monclair, P.F. Ambros, G.M. Brodeur, A. Faldum, B. Hero, T. Iehara, D. Machin, V. Mosseri, T. Simon, A. Garaventa, V. Castel, K.K. Matthay, I.T. Force, The international neuroblastoma risk group (INRG) classification system: An INRG task Force report. *J Clin Oncol* **27**, 289–297 (2009)
2. J.M. Maris, Recent advances in neuroblastoma. *N Engl J Med* **362**, 2202–2211 (2010)
3. C.P. Reynolds, K.K. Matthay, J.G. Villablanca, B.J. Maurer, Retinoid therapy of high-risk neuroblastoma. *Cancer Lett* **197**, 185–192 (2003)
4. K.K. Matthay, C.P. Reynolds, R.C. Seeger, H. Shimada, E.S. Adkins, D. Haas-Kogan, R.B. Gerbing, W.B. London, J.G. Villablanca, Long-term results for children with high-risk neuroblastoma treated on a randomized trial of myeloablative therapy followed by 13-cis-retinoic acid: A children's oncology group study. *J Clin Oncol* **27**, 1007–1013 (2009)
5. S. Hatakeyama, TRIM proteins and cancer. *Nat Rev Cancer* **11**, 792–804 (2011)
6. B. Le Douarin, C. Zechel, J.M. Garnier, Y. Lutz, L. Tora, P. Pierrat, D. Heery, H. Gronemeyer, P. Chambon, R. Losson, The N-terminal part of TIF1, a putative mediator of the ligand-dependent activation function (AF-2) of nuclear receptors, is fused to B-raf in the oncogenic protein T18. *EMBO J* **14**, 2020–2033 (1995)
7. B. Le Douarin, A.L. Nielsen, J.M. Garnier, H. Ichinose, F. Jeanmougin, R. Losson, P. Chambon, A possible involvement of TIF1 alpha and TIF1 beta in the epigenetic control of transcription by nuclear receptors. *EMBO J* **15**, 6701–6715 (1996)
8. W.W. Tsai, Z. Wang, T.T. Yiu, K.C. Akdemir, W. Xia, S. Winter, C.Y. Tsai, X. Shi, D. Schwarzer, W. Plunkett, B. Aronow, O. Gozani, W. Fischle, M.C. Hung, D.J. Patel, M.C. Barton, TRIM24 links a non-canonical histone signature to breast cancer. *Nature* **468**, 927–932 (2010)
9. L.H. Zhang, A.A. Yin, J.X. Cheng, H.Y. Huang, X.M. Li, Y.Q. Zhang, N. Han, X. Zhang, TRIM24 promotes glioma progression and enhances chemoresistance through activation of the PI3K/Akt signaling pathway. *Oncogene* **34**, 600–610 (2015)
10. D. Lv, Y. Li, W. Zhang, A.A. Alvarez, L. Song, J. Tang, W.Q. Gao, B. Hu, S.Y. Cheng, H. Feng, TRIM24 is an oncogenic transcriptional co-activator of STAT3 in glioblastoma. *Nat Commun* **8**, 1454 (2017)
11. G. Zhao, C. Liu, X. Wen, G. Luan, L. Xie, X. Guo, The translational values of TRIM family in pan-cancers: From functions and mechanisms to clinics. *Pharmacol Ther* **227**, 107881 (2021)
12. K. Allton, A.K. Jain, H.M. Herz, W.W. Tsai, S.Y. Jung, J. Qin, A. Bergmann, R.L. Johnson, M.C. Barton, Trim24 targets

- endogenous p53 for degradation. *Proc Natl Acad Sci U S A* **106**, 11612–11616 (2009)
13. A.C. Groner, L. Cato, J. de Tribolet-Hardy, T. Bernasocchi, H. Janouskova, D. Melchers, R. Houtman, A.C.B. Cato, P. Tschopp, L. Gu, A. Corsinotti, Q. Zhong, C. Fankhauser, C. Fritz, C. Poyet, U. Wagner, T. Guo, R. Aebersold, L.A. Garraway, et al., TRIM24 is an oncogenic transcriptional activator in prostate Cancer. *Cancer Cell* **29**, 846–858 (2016)
 14. K. Khetchoumian, M. Teletin, J. Tisserand, M. Mark, B. Herquel, M. Ignat, J. Zucman-Rossi, F. Cammas, T. Lerouge, C. Thibault, D. Metzger, P. Chambon, R. Losson, Loss of Trim24 (Tif1alpha) gene function confers oncogenic activity to retinoic acid receptor alpha. *Nat Genet* **39**, 1500–1506 (2007)
 15. J. Tisserand, K. Khetchoumian, C. Thibault, D. Dembele, P. Chambon, R. Losson, Tripartite motif 24 (Trim24/Tif1alpha) tumor suppressor protein is a novel negative regulator of interferon (IFN)/signal transducers and activators of transcription (STAT) signaling pathway acting through retinoic acid receptor alpha (Raralpha) inhibition. *J Biol Chem* **286**, 33369–33379 (2011)
 16. H. Feng, B. Hu, K.W. Liu, Y. Li, X. Lu, T. Cheng, J.J. Yiin, S. Lu, S. Keezer, T. Fenton, F.B. Furnari, R.L. Hamilton, K. Vuori, J.N. Sarkaria, M. Nagane, R. Nishikawa, W.K. Cavenee, S.Y. Cheng, Activation of Rac1 by Src-dependent phosphorylation of Dock180(Y1811) mediates PDGFRalpha-stimulated glioma tumorigenesis in mice and humans. *J Clin Invest* **121**, 4670–4684 (2011)
 17. Y. Hu, G.K. Smyth, ELDA: Extreme limiting dilution analysis for comparing depleted and enriched populations in stem cell and other assays. *J Immunol Methods* **347**, 70–78 (2009)
 18. K.W. Liu, H. Feng, R. Bachoo, A. Kazlauskas, E.M. Smith, K. Symes, R.L. Hamilton, M. Nagane, R. Nishikawa, B. Hu, S.Y. Cheng, SHP-2/PTPN11 mediates gliomagenesis driven by PDGFRA and INK4A/ARF aberrations in mice and humans. *J Clin Invest* **121**, 905–917 (2011)
 19. G. Yu, L.-G. Wang, Y. Han, Q.-Y. He, clusterProfiler: An R package for comparing biological themes among gene clusters. *OMICS* **16**, 284–287 (2012)
 20. N.J. Balamuth, A. Wood, Q. Wang, J. Jagannathan, P. Mayes, Z. Zhang, Z. Chen, E. Rappaport, J. Courtright, B. Pawel, B. Weber, R. Wooster, E.O. Sekyere, G.M. Marshall, J.M. Maris, Serial transcriptome analysis and cross-species integration identifies centromere-associated protein E as a novel neuroblastoma target. *Cancer Res* **70**, 2749–2758 (2010)
 21. I. Janoueix-Lerosey, D. Lequin, L. Brugières, A. Ribeiro, L. de Pontual, V. Combaret, V. Raynal, A. Puisieux, G. Schleiermacher, G. Pierron, D. Valteau-Couanet, T. Frebourg, J. Michon, S. Lyonnet, J. Amiel, O. Delattre, Somatic and germline activating mutations of the ALK kinase receptor in neuroblastoma. *Nature* **455**, 967–970 (2008)
 22. P. Rajbhandari, G. Lopez, C. Capdevila, B. Salvatori, J. Yu, R. Rodriguez-Barrueco, D. Martinez, M. Yarmarkovich, N. Weichert-Leahey, B.J. Abraham, M.J. Alvarez, A. Iyer, J.L. Harenza, D. Oldridge, K. De Preter, J. Koster, S. Asgharzadeh, R.C. Seeger, J.S. Wei, et al., Cross-cohort analysis identifies a TEAD4-MYCIN positive feedback loop as the Core regulatory element of high-risk neuroblastoma. *Cancer Discov* **8**, 582–599 (2018)
 23. S.M.-I. Consortium, A comprehensive assessment of RNA-seq accuracy, reproducibility and information content by the sequencing quality control consortium. *Nat Biotechnol* **32**, 903–914 (2014)
 24. X. Han, B. Gui, C. Xiong, L. Zhao, J. Liang, L. Sun, X. Yang, W. Yu, W. Si, R. Yan, X. Yi, D. Zhang, W. Li, L. Li, J. Yang, Y. Wang, Y.E. Sun, D. Zhang, A. Meng, Y. Shang, Destabilizing LSD1 by Jade-2 promotes neurogenesis: An antibraking system in neural development. *Mol Cell* **55**, 482–494 (2014)
 25. S. Amente, G. Milazzo, M.C. Sorrentino, S. Ambrosio, G. Di Palo, L. Lania, G. Perini, B. Majello, Lysine-specific demethylase (LSD1/KDM1A) and MYCN cooperatively repress tumor suppressor genes in neuroblastoma. *Oncotarget* **6**, 14572–14583 (2015)
 26. M.G. Lee, C. Wynder, N. Cooch, R. Shiekhattar, An essential role for CoREST in nucleosomal histone 3 lysine 4 demethylation. *Nature* **437**, 432–435 (2005)
 27. J. Wysocka, T.A. Milne, C.D. Allis, Taking LSD 1 to a new high. *Cell* **122**, 654–658 (2005)
 28. B. Lakowski, I. Roelens, S. Jacob, CoREST-like complexes regulate chromatin modification and neuronal gene expression. *J Mol Neurosci* **29**, 227–239 (2006)
 29. Y. Song, L. Dagil, L. Fairall, N. Robertson, M. Wu, T.J. Ragan, C.G. Savva, A. Saleh, N. Morone, M.B.A. Kunze, A.G. Jamieson, P.A. Cole, D.F. Hansen, J.W.R. Schwabe, Mechanism of crosstalk between the LSD1 demethylase and HDAC1 deacetylase in the CoREST complex. *Cell Rep* **30**, 2699–2711 (2020)
 30. J.H. Schulte, S. Lim, A. Schramm, N. Friedrichs, J. Koster, R. Versteeg, I. Ora, K. Pajtler, L. Klein-Hitpass, S. Kuhfittig-Kulle, E. Metzger, R. Schule, A. Eggert, R. Buettner, J. Kirfel, Lysine-specific demethylase 1 is strongly expressed in poorly differentiated neuroblastoma: Implications for therapy. *Cancer Res* **69**, 2065–2071 (2009)
 31. N. Bayeva, E. Coll, O. Piskareva, Differentiating neuroblastoma: A systematic review of the retinoic acid, its derivatives, and synergistic interactions. *J Pers Med* **11**, 211 (2021)
 32. K. Chen, Y. Cai, C. Cheng, J. Zhang, F. Lv, G. Xu, P. Duan, Y. Wu, Z. Wu, MYT1 attenuates neuroblastoma cell differentiation by interacting with the LSD1/CoREST complex. *Oncogene* **39**, 4212–4226 (2020)
 33. Y.J. Shi, C. Matson, F. Lan, S. Iwase, T. Baba, Y. Shi, Regulation of LSD1 histone demethylase activity by its associated factors. *Mol Cell* **19**, 857–864 (2005)
 34. T. Schenk, W.C. Chen, S. Gollner, L. Howell, L. Jin, K. Hebestreit, H.U. Klein, A.C. Popescu, A. Burnett, K. Mills, R.A. Casero Jr., L. Marton, P. Woster, M.D. Minden, M. Dugas, J.C. Wang, J.E. Dick, C. Muller-Tidow, K. Petrie, A. Zelent, Inhibition of the LSD1 (KDM1A) demethylase reactivates the all-trans-retinoic acid differentiation pathway in acute myeloid leukemia. *Nat Med* **18**, 605–611 (2012)
 35. K. Khetchoumian, M. Teletin, J. Tisserand, B. Herquel, K. Ouarhni, R. Losson, Trim24 (Tif1 alpha): An essential 'brake' for retinoic acid-induced transcription to prevent liver cancer. *Cell Cycle* **7**, 3647–3652 (2008)
 36. W.S. Palmer, G. Poncet-Montange, G. Liu, A. Petrocchi, N. Reyna, G. Subramanian, J. Theroff, A. Yau, M. Kost-Alimova, J.P. Bardenhagen, E. Leo, H.E. Shepard, T.N. Tieu, X. Shi, Y. Zhan, S. Zhao, M.C. Barton, G. Draetta, C. Toniatti, et al., Structure-guided design of IACS-9571, a selective high-affinity dual TRIM24-BRPF1 Bromodomain inhibitor. *J Med Chem* **59**, 1440–1454 (2016)
 37. L.N. Gechijian, D.L. Buckley, M.A. Lawlor, J.M. Reyes, J. Paulk, C.J. Ott, G.E. Winter, M.A. Erb, T.G. Scott, M. Xu, H.S. Seo, S. Dhe-Paganon, N.P. Kwiatkowski, J.A. Perry, J. Qi, N.S. Gray, J.E. Bradner, Functional TRIM24 degrader via conjugation of ineffectual bromodomain and VHL ligands. *Nat Chem Biol* **14**, 405–412 (2018)
 38. M. Han, Y. Sun, Pharmacological targeting of tripartite motif containing 24 for the treatment of glioblastoma. *J Transl Med* **19**, 505 (2021)
 39. V.V. Shah, A.D. Duncan, S. Jiang, S.A. Stratton, K.L. Allton, C. Yam, A. Jain, P.M. Krause, Y. Lu, S. Cai, Y. Tu, X. Zhou, X. Zhang, Y. Jiang, C.L. Carroll, Z. Kang, B. Liu, J. Shen, M.

Gagea, et al., Mammary-specific expression of Trim24 establishes a mouse model of human metaplastic breast cancer. *Nat Commun* **12**, 5389 (2021)

Publisher's note Springer Nature remains neutral with regard to jurisdictional claims in published maps and institutional affiliations.

Springer Nature or its licensor (e.g. a society or other partner) holds exclusive rights to this article under a publishing agreement with the author(s) or other rightsholder(s); author self-archiving of the accepted manuscript version of this article is solely governed by the terms of such publishing agreement and applicable law.